International Journal of Engineering Innovation & Research
Volume 3, Issue 3, ISSN: 2277 – 5668

Radiation from Circular Array of Polyethylene Dielectric Rod Antennas

Dr. M. V. S. Prasad
Professor, Dept of ECE,
R.V.R. & J.C.College of Engg., Guntur
Email: mvs_prasad67@yahoo.co.in

D. Asha.
M.Tech., Dept of ECE,
R.V.R. & J.C.College of Engg., Guntur

M. Himaja
Final Year B. Tech., Dept of ECE,
R.V.R. & J.C.College of Engg., Guntur

Abstract – **Computational studies were performed on circular arrays using tapered Polyethylene (ε_r =2.3) dielectric rod antennas, of length (L) equal to $3\lambda_0$ and taper angle (θ_1) equal to 4°, as radiating elements and their results are presented in this paper. The objective of the computational study is to find the best possible number of elements in the array. The Polyethylene dielectric rod antennas are uniformly spaced around the circumference of a circle without overlap between the elements. The number of radiating elements in the array is varied from 4 to 40, with an increase of 4 elements. The principal plane patterns are computed, using the principle of pattern multiplication. For each set of elements, Half Power Beam Width (HPBW), Side Lobe Level (SLL), and Directivity (D_0) are determined. The principle plane patterns are presented for the best possible number of elements in the array.**

Keywords – **Polyethylene Rod Antenna, Taper Angle, Circular Array, Array Factor, Directivity, Side Lobe Level, Half Power Beam Width.**

I. Introduction

In a circular array, the radiating elements are placed along the circumference of a circle with uniform spacing. These arrays find wide applications in radio direction finding, air and space navigation, radar and sonar systems [1]. Several investigations has been carried out using circular arrays using with different types of radiating elements and are reported in literature [2]-[5]. The main feature of the circular array that is seen in most of the applications is the scanning of the main beam through 360° in the azimuthal plane (plane of the array). However, by proper choice of the elements, their orientation and phase excitation it is possible to obtain a main beam in the direction of zenith and scan it over a small angle cone, around the zenith direction, with a little change of either beam width or side lobe level. The selection of Polyethylene rod antenna of length $3\lambda_0$ and taper angle 4°, is made on the basis of the results of computational studies, carried out on the radiation patterns of tapered Polyethylene rod antennas, reported in [6]. In this paper, the results of computational studies of the radiation patterns, of a circular array of tapered Polyethylene dielectric rod antennas are presented.

II. Radiation from Tapered Polyethylene Rod Antenna

The radiation from a dielectric rod antenna mainly depends on the dielectric material used to fabricate the antenna, physical dimension of the antenna, and the method of excitation of the antenna. The dielectric rod antenna is excited in the hybrid HE_{11} mode. The advantage of asymmetric HE_{11} mode is that it gives maximum radiation in the axial direction and it does not shows any cut off behavior.

The amplitude of side lobes and back lobes may be reduced, by tapering the dielectric rod antenna, until the diameter is reached for which the wave impedance becomes equal to that of free space impedance. Tapering the dielectric rod minimizes the standing wave distribution caused by reflection at the free end of the rod and the electric field distribution rises to maximum near the midpoint of the length of the rod and then falls off towards the free end [7].

The electric fields radiated by a tapered dielectric rod antenna are analyzed by Anand Kumar and Rajeswari Chatterjee using the Schelkunoff's equivalence principle [8]. The principle states that the electromagnetic field inside a surface S, due to sources outside the surface can be produced by sheet electric currents **J** and sheet magnetic currents **M** over the surface S given by the following equations,

$$\mathbf{J} = -\hat{\mathbf{n}} \times \mathbf{H}^{\circ} \quad (1)$$

$$\mathbf{M} = \hat{\mathbf{n}} \times \mathbf{E}^{\circ} \quad (2)$$

where $\hat{\mathbf{n}}$ is a unit normal vector directed outwards from S, $\mathbf{E}^{\circ}$ and $\mathbf{H}^{\circ}$ are the values of **E** and **H** on the surface S. The geometry of tapered dielectric rod is shown in Fig.1. Following the analysis in [8], the electric field components radiated by a tapered dielectric rod are given by:

$$\begin{aligned}\left(\frac{2\lambda_0 r}{A}\right) j \exp\,(j\beta_0 r)\, E_\theta = \\ -j\,(1/f\varepsilon_1)\, \sin\,\varphi\varphi_1 + j\,(1/2\, f\varepsilon_1)\, \cos\varphi\, \sin 2\varphi\, I_2 \\ -j\,(\lambda_0/2)\, \cos\theta\, \cos\varphi\, \sin 2\varphi\, I_3 \\ -j\lambda_0 \cos\theta \sin\varphi I_4 + j\, 2\pi\eta_0\, \sin\theta \sin\varphi\, I_6 \\ -\pi\, ((1+\delta_l\eta_1^e) + [(\beta_l/\beta_0) + \eta_0\delta_l]\, \cos\theta)\, \exp(j\beta_l l) \sin\varphi I_7 \\ -\pi\, ((1\text{-}\delta_l\eta_1^e) + [(\beta_l/\beta_0)\text{-}\eta_0\delta_l]\, \cos\theta)\, \exp(j\beta_l l) \sin\varphi I_8\end{aligned} \quad (3)$$

and

International Journal of Engineering Innovation & Research
Volume 3, Issue 3, ISSN: 2277 – 5668

$$\left(\frac{2\lambda_0 r}{A}\right) j\ \exp\ (j\beta_0 r)\ E_\varphi =$$
$$-j\,(1/f\varepsilon_1)\ \cos\ \theta\theta\cos\ \varphi\varphi_1 - j\,(1/2\,f\varepsilon_1)\ \cos\theta\ \sin\varphi\sin 2\varphi\ I_2$$
$$+\ j\,(\lambda_0/2)\ \sin\varphi\ \sin 2\varphi\ I_3 - j\,\lambda_0\ \cos\varphi\ I_4 + j\ 2\pi\ \sin\theta\cos\varphi\ I_5$$
$$+\pi\ ((1+\delta_l\eta_1^e)\ \cos\ \theta + [(\beta_l/\beta_0)+\eta_0\delta_l])\ \exp(j\beta_l l)\ \cos\varphi I_7$$
$$+\pi\ ((1\text{-}\delta_l\eta_1^e)\ \cos\ \theta + [(\beta_l/\beta_0)\text{-}\eta_0\delta_l])\ \exp(j\beta_l l)\ \cos\varphi I_8$$

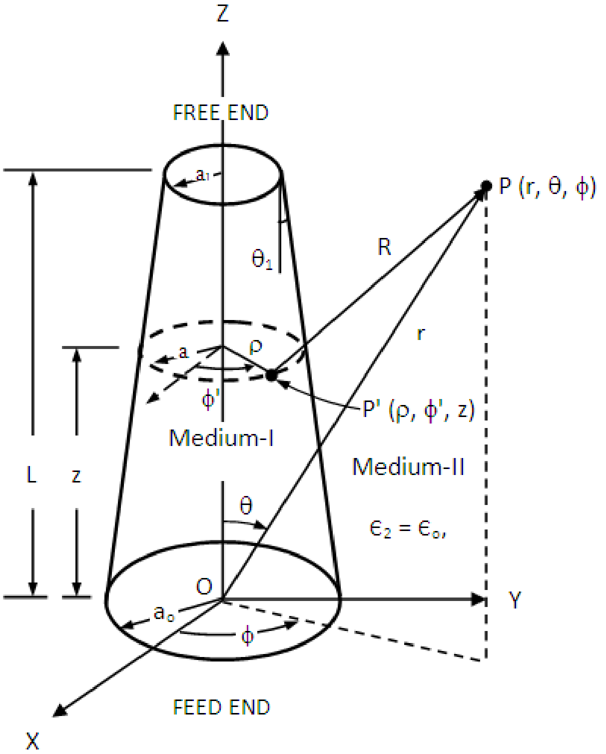

Fig.1. Geometry of tapered dielectric rod antenna

where A is the excitation constant for H modes and

$$I_1 = \int_0^L \exp(j\beta z)\ \delta r J_1(r)\left\{\sin^2\phi\, J_o(\xi) + \cos 2\phi\,[J_1(\xi)/\xi]\right\} dz \quad (5)$$

$$I_2 = \int_0^L \exp(j\beta z)\,\delta\, k_1 r J_1(r)\left[2\frac{J_1(\xi)}{\xi} - J_0(\xi)\right] dz \quad (6)$$

$$I_3 = \int_0^L \exp(j\beta z)\, k_1 r J_1(r)\left[2\frac{J_1(\xi)}{\xi} - J_0(\xi)\right] dz \quad (7)$$

$$I_4 = \int_0^L \exp(j\beta z)\, k_1 r J_1(r)\left[\cos^2\phi\, J_0(\xi) - \cos 2\phi\,\frac{J_1(\xi)}{\xi})\right] dz \quad (8)$$

$$I_5 = \int_0^L \exp(j\beta z)\left[r J_0(r) - (1-\delta\eta_1^e) J_1(r)\right] J_1(\xi)\, dz \quad (9)$$

$$I_6 = \int_0^L \exp(j\beta z)\left[\delta r J_0(r) + \left(\frac{1}{\eta_1^m} - \delta\right) J_1(r)\right] J_1(\xi)\, dz \quad (10)$$

$$I_7 = \int_0^{a_1} R\, J_0(R)\, J_0(\xi_1)\, d\rho \quad (11)$$

$$I_8 = \int_0^{a_1} [2J_1(R) - RJ_0(R)]\left[2\frac{J_1(\xi_1)}{\xi_1} - J_0(\xi_1)\right] d\rho \quad (12)$$

with $\xi = \beta_o$ a sin θ and $\xi_1 = \beta_o\ \rho \sin\theta$

In (3) - (10), δ is the ratio of excitation constants for E and H modes. The values of δ and k_1 may be computed, by representing their variation given in Fig.2 of [8], by piecewise linear models as:

$\delta=0.007$ for $a/\lambda_0 \leq 0.1$ (13)

$\delta=(2.9-a/\lambda_0)/400$ for $a/\lambda_0 \geq 0.1$ (14)

and

$k_1 = 0.5\ (15 - a/\lambda_0)$ for $a/\lambda_0 \leq 0.2$ (15)

$k_1 = 0.2\ (15 - 17\ a/\lambda_0)$ for $a/\lambda_0 \geq 0.2$ (16)

δ_1 is the value of δ at z = L in Fig.1.

The H-plane pattern may be obtained by setting $\phi = 0^\circ$, and the E-plane pattern by setting $\phi = 90^\circ$ in (3) and (4).

III. Array Factor of Circular Array

The circular array of isotropic radiators is shown in Fig.2. Radius of the circle, ρ_1 is

$$\rho_1 = N\lambda_0 / 2\pi \quad (17)$$

where N is the number of elements in the array and λ_0 is the wavelength.

Elements are placed at azimuthal angular intervals of 2π / N. The azimuthal angle ϕ_n of the n[th] element is

$$\phi_n = \frac{2\pi n}{N} \quad (18)$$

Array factor, AF, of a circular array of N equally spaced elements may be written [1] as

$$AF = \sum_{n=1}^{N} I_n \exp\left\{j\left[\beta_0\rho_1 \sin\theta\cos\left(\phi\text{-}\phi_n\right) + \alpha_n\right]\right\} \quad (19)$$

where I_n = amplitude excitation of the n[th] element,

α_n = phase excitation of the n[th] element,

and $\beta_0 = 2\pi / \lambda_0$ is the phase constant.

For uniform amplitude excitation of each element $I_n = I_o$, a constant. To direct the maximum of the main beam in the (θ_o, ϕ_o) direction, α_n may be chosen to be

$$\alpha_n = -\beta_0\rho_1 \sin\theta\cos(\phi_0 - \phi_n) \quad (20)$$

In Fig.2, $R_n = r - \rho_1\cos(\psi_n)$ (21)

where r is the distance from origin to point 'P', ρ_1 is radius of circle, and ψ_n is the progressive phase between the elements in the array.

IV. Circular Array of Polyethylene Rod Antennas

The tapered Polyethylene rod antennas, with feed end diameter equal to 0.025m are used as radiating elements in the array. The elements are uniformly spaced with a centre to centre spacing of λ_0 m between the elements. The radius of the array to place N number of elements without overlapping is then given by

$$\rho_1 = N\lambda_0 / 2\pi \quad (22)$$

with this radius, the array factor can be computed using(19).

Total field, **E**, of the array can be computed using the principle of pattern multiplication as:

E = **E** (Field of Single element) × Array Factor (23)

The components of **E** radiated by a single Polyethylene rod antenna are given by (3) and (4) and the array factor is given by (19). The principle plane patterns are computed using (23).

Software has been implemented in matlab to plot the radiation patterns.

V. Results and Discussion

Circular array of tapered Polyethylene rod antennas of length (L) equal to $3\lambda_0$, and taper angle (θ_1) equal to 4° is considered, to compute the principal plane patterns of the array at a frequency of 10 GHz or λ_0=0.03m. The elements are uniformly placed around the circumference of the circle. The number of elements is varied from 4 to 40 with an increase of 4. The principal plane patterns are computed for each set of elements and HPBW, SLL, and D_0 are computed for each set of elements and results are presented in Table-1.The Directivity may be computed using Kraus's formula [1]:

$$\text{Directivity}\,(D_0) = 41253/\ (\theta_E \times \theta_H) \qquad (24)$$

Where θ_E = HPBW in E-Plane (degrees)

θ_H = HPBW in H-Plane (degrees)

From the results presented in Table-1, it may be observed that, with increasing number of elements in the array the directivity as well as side lobe level increase, and it may also be observed that N=12, may be considered as best possible number of elements, because in this case directivity is 26.16 dB and side lobe level is -10.46 dB. In all other cases, even though directivity is high, the SLL is slightly higher compared with N=12 case. For moderate directivities the number of elements N= 8 may be used because in this case SLL is very low i.e. -14.42dB. From the results it is also observed that as the number of elements increases Directivity also increases. The principle plane patterns for best possible number of elements are shown in Fig.3.

With a directivity of 26.16 dB and side lobe level of -10.46 dB, this array may be an attractive choice for radar applications.

Table 1: Variation of Radius of Array, HPBW, SLL, and D_0 with number of elements

S. No.	Number of Elements (N)	Radius of array in Cm	HPBW (Deg.)		SLL (dB)		D_0 (dB)
			$\phi=0^\circ$	$\phi=90^\circ$	$\phi=0^\circ$	$\phi=90^\circ$	
1	4	1.91	25	25	-40	-40	18.19
2	8	3.81	15.6	16	-14.42	-13.98	22.18
2	12	5.73	10.4	9.6	-10.46	-10.17	26.16
3	16	7.62	7.8	8	-9.49	-9.37	28.2
4	20	9.54	6.6	6.4	-8.87	-8.83	29.89
5	24	11.43	5.2	5.6	-8.64	-8.52	31.51
6	28	13.35	4.6	4.8	-8.52	-8.4	32.71
7	32	15.27	4	4.2	-8.17	-8.07	33.9
8	36	15.81	3.6	4.4	--8.18	-7.96	34.16
9	40	19.11	3	3.1	-8.75	-8.87	36.47

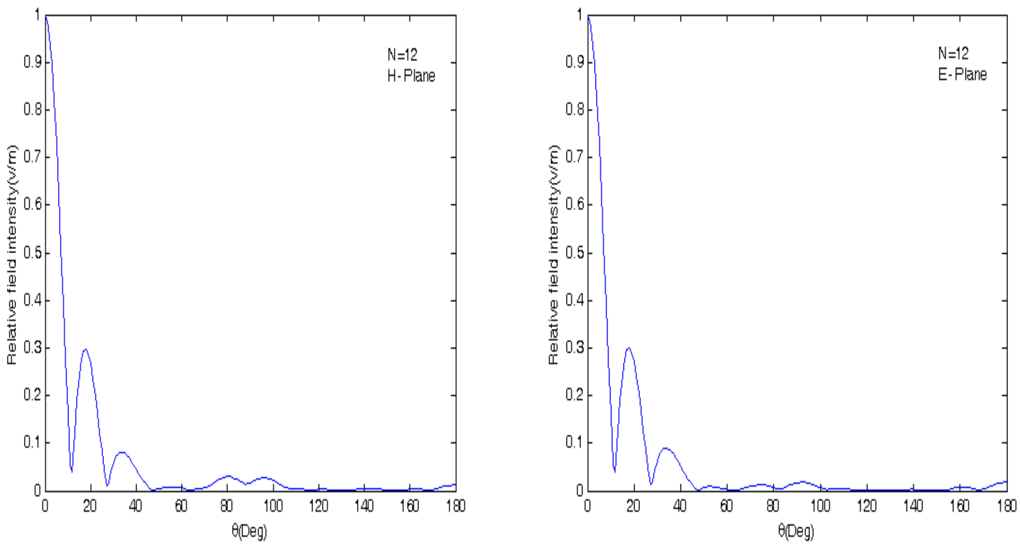

Fig.3. Principal Plane patterns of circular array (N=12).

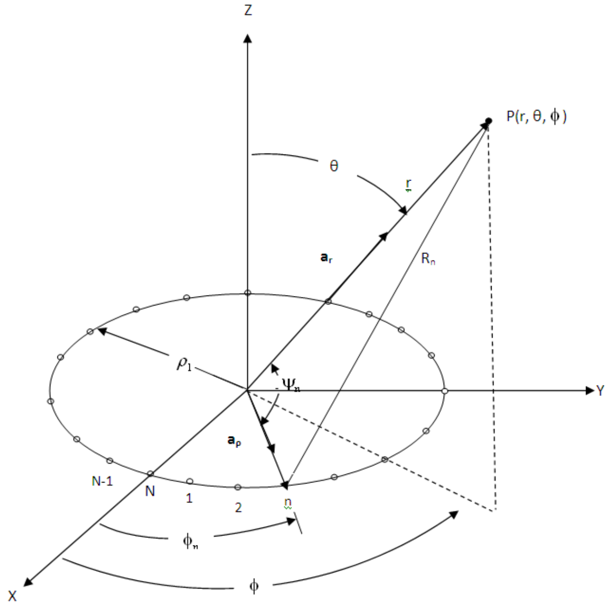

Fig.2. Geometry of circular array of N elements

REFERENCES

[1] Constantine A.Balanis, "Antenna Theory Analysis and Design", 2nd edition, John wiley & Sons Inc., pp 324-328. 2002.

[2] Rodney G.Vaughan, J.Bach Anderson and M.H.Langhorn, "Circular array of outward sloping monopoles for Vehicular Diversity Antennas", IEEE Trans. Antennas propagation, Vol.36, No.10, pp 1365-1374. 1988.

[3] Ronaold W.P.King, "Supergain antennas and the Yagi and circular arrays", IEEE Trans. Antennas propagation, Vol.37, No.2, pp178-186. 1989.

[4] Song Lizhong, Maning, Li Chongshen and Wuqum, "simulation and analysis of a microstrip circular array antenna at 15 GHz", IEEE Xplore, 2008.

[5] Naveen kumar sexena and Dr.P.K.S.Pourush, , "Circular array of Triangular patches as filter", IEEE Xplore. 2009.

[6] Dr.M.V.S.Prasad, Dr.R.V.S.Satyanarayana, P.Srilakshmi "Computational Studies on Tapered Polyethylene Rod Antennas", International Journal of Electronics and communication Engineering, pp. 143-152, Volume 6, Number 1, 2013.

[7] D.G. Kiely, "Dielectric Aerials", 1st edition, Mathuen & Co Limited, London, page 41. 1953.

[8] Anand Kumar, R.Chatterjee, "Radiation from tapered Dielectric Rod Aerials", IISC Journal, vol.50, issue no.4, pp. 374-392. 1968.

AUTHOR PROFILE

Dr. M. V. S. Prasad

is having 22 years of teaching experience. Presently, he is working as a professor in the department of ECE of R.V.R & J.C College of Engineering Guntur, A.P. He obtained his Bachelor's degree in ECE and Masters degree in Electronics and Instrumentation from Andhra University Vizag in the year 1989 and 1999. He obtained his Doctorate Degree from Sri Venkateswara University Tirupati in the year 2012 and he published several research papers in National and International Journals. His interesting fields are Antennas, Microwaves, electronic circuits and EMC/EMI.

He received Best Paper award in the National Conference organized by S.V.University College of Engineering and IETE Tirupati centre during January 2012. He worked as Honorable Secretary during 2010 - 2012 for IETE Vijayawada centre. He is life member in ISTE, EMC (Electromagnetic Compatibility) society and Fellow of IETE.